International Journal of GEOMATE, Jan., 2023, Vol.24, Issue 101, pp.84-93
ISSN: 2186-2982 (P), 2186-2990 (O), Japan, DOI: https://doi.org/10.21660/2023.101.g12224
Geotechnique, Construction Materials and Environment

EFFECTS OF TEMPERATURE ON STRENGTH AND TIME-DEPENDENT DEFORMATION BEHAVIOURS OF HOSTUN SAND UNDER SHEAR

Kosit Jariyatatsakorn[1] and *Warat Kongkitkul[2]

[1,2]Department of Civil Engineering, Faculty of Engineering, King Mongkut's University of Technology Thonburi, Thailand

*Corresponding Author, Received: 14 June 2022, Revised: 26 Dec. 2022, Accepted: 10 Jan. 2023

ABSTRACT: Hostun sand is widely adopted as a standard sand used in various laboratory stress-strain tests in geotechnical engineering research. In this study, the effects of temperature on the shear strength and time-dependent deformation behaviours of Hostun sand are of interest. A comprehensive series of temperature-controlled triaxial compression tests were performed on air-dried Hostun sand sample. During the drained heating stage, the sample was heated to different target temperatures (i.e., 30, 45 and 60°C), after which the temperature was held constant. Then, the sample was sheared under constant cell pressure and temperature. Small strain-amplitude cyclic loading and sustained loading were successively applied at different shear stress levels for investigating equivalent elastic Young's modulus (E_{eq}) and creep behaviour. The following were found. Shear strengths, both at the peak sand residual stages, decrease with increasing temperature. The E_{eq} increases with increasing shear stress level, but at the same shear stress level, it decreases with increasing temperature. The E_{eq} can be expressed as a function of the shear stress level and temperature. The axial creep strain increases with increasing shear stress level and temperature.

Keywords: Creep, Elasticity, Hostun sand, Temperature, Triaxial compression test

1. INTRODUCTION

Many geotechnical engineering-related structures are subjected to temperature change, for example, energy piles [1]-[4], energy-efficient techniques for space heating and cooling via borehole heat exchangers (BHE) [5], thermally-active mechanical stabilized earth walls with additional plumbing for heat exchange [6], nuclear waste disposal [7], etc. Therefore, in these circumstances, the surrounding soil and reinforcement are subjected to non-isothermal conditions. In the previous studies, number of research on the thermo-mechanical behaviour of clay under various temperature-controlled tests has gradually increased over the years. These studies were conducted by performing triaxial compression (TC), one-dimensional compression, or isotropic compression [8]-[11]. Conversely, the thermal effect on the behaviour of granular materials, especially sand, has been rarely reported, for example, stress-strain behaviour of densely compacted sand at high pressure and temperature to fill the containers of waste nuclear fuel, thermal effect on the shear strength and volume change behaviour of saturated sand [12]-[14]. Moreover, the temperature effect combining with the time effect (e.g., creep behaviour) has rarely been comprehensively investigated.

For predicting long-term settlement or secondary consolidation, the classical consolidation theory is commonly applied to determine the settlement of soils. In fact, the deformation of the soils has occurred as not only elastic deformation but also inelastic deformation. The increment of inelastic strain is developed by plastic yielding that is controlled by the viscous effect and inviscid cyclic loading effect [15]. Therefore, to precisely predict the long-term deformation of soils, both elastic and viscous properties should be concerned.

The elastic properties of geomaterials were investigated with various aspects by plenty of studies. For example, Hoque and Tatsuoka [16] performed a series of triaxial tests with large-size specimens on various granular materials (e.g., Toyoura sand, Hostun sand, Ticino sand) and found that elasticity is a stress-dependent property. The test results agree well with the one of Kohata et al. [17], in which the triaxial tests on small-size air-dried Hostun sand were performed. Moreover, a pair of local deformation transducers (LDTs) were attached to the surface of the specimen for precise measurement of axial strain to compare with the elastic modulus obtained from an external measurement. Duttine et al. [18] studied the anisotropic small-strain elastic properties of Hostun and Toyoura sands by triaxial compression test. The elastic properties were measured by both static and dynamic methods (i.e., small cyclic loadings and shear, and compression wave propagations). The

test results showed that the elastic properties are non-linearly related to stress state for both Hostun and Toyoura sands. Thus, the elastic property from numerous previous studies is stress state-dependent or it can be understood that the elastic property exhibited a hypo-elastic manner. Nevertheless, the study of elastic property with the temperature effect are rarely limited. Mitchell [19] showed that the elastic modulus of most engineering materials is temperature dependent. Therefore, the elastic behaviours of geomaterials are likely temperature-dependent too. Punya-in and Kongkitkul [20] performed a series of triaxial compression tests on a clean sand. The elastic property was evaluated in terms of E_{eq} by performing small unload-reload cycles after SL test. The results revealed that the E_{eq} decreased with increasing temperature. However, in the past studies, the thermal effect on the elastic modulus of geomaterials was still ambiguous because of different experimental conditions (e.g., the studies of Cekerevac and Laloui, Liu et al., and Murayama [9], [13], [22]). Enomoto et al. [23] revealed that the creep deformation depends on loading rate, particle shape, stress level and so on. These factors can be explained by the viscous properties of geomaterials. Tatsuoka et al. [24] explained the creep deformation as a response by the viscous properties of geomaterials with an aid of non-linear three-component (NTC) model.

However, the studies of thermal effect on creep behaviour of geomaterials are limited. For example, Tsutsumi and Tanaka [11] investigated the combined effects of temperature and strain rate on clayey soils and found that the clay specimen exhibited peculiar viscous behaviour (i.e., non-isotach viscosity type) when the temperature was high and the strain rate was low. In addition, Kaddouri et al. [25] performed a series of creep tests by using the temperature-controlled oedometer on a saturated compacted clayey soil. The test results showed that the creep deformation increases with increasing stress level and temperature.

2. RESEARCH SIGNIFICANCE

As mentioned in the previous section, it can be readily seen that the elastic and creep behaviour of sand with the temperature effect are rarely limited and still ambiguous. Therefore, the aim of this study focused on the investigation of elastic and creep behaviour with temperature effect of Hostun sand. the creep deformation and elastic Young's modulus of Hostun sand were investigated in temperature-controlled triaxial compression test. Air-dried sand specimens were used in this study to eliminate the difference of thermal expansion between the solid and liquid in the specimen, and to avoid the pore pressure induced by the heating, consolidation, and shearing stages.

The elastic properties were presented in terms of E_{eq} by performing the CL test, while the creep strain was obtained by performing SL test at different stress levels and temperatures.

3. MATERIAL AND TEST APPARATUS

3.1 Test Material

Hostun sand is widely adopted in the geotechnical engineering research in France. The particle shape is sub-angular to angular. It has specific gravity (G_s) of 2.584, an effective particle size (D_{50}) of 0.302 mm, and a coefficient of uniformity (C_u) of 1.999. The maximum and minimum void ratios are 0.854 and 0.522, respectively, which are determined in accordance with JIS A 1224:2009 [26]. Its gradation curve, index properties, and particle shape are shown in Fig. 1.

3.2 Test Apparatus

A temperature-controlled triaxial compression test apparatus (Fig. 2) used in this study was developed by Punya-in and Kongkitkul [20]. The temperature was measured by two sets of the k-type thermocouple. One of them was installed inside the triaxial cell for measuring the temperature surrounding the specimen (No.⑥ in Fig. 2), and the other (No.⑤ in Fig. 2) at the outflow of thermal controller for the feedback control of the circulating water. The temperature value measured at No. ⑥ was recorded by a computer. The cell water temperature was elevated to the target value by using a heater and a pair of diaphragm pumps, which were used to circulate the cell water. The cell pressure is automatically controlled by an electro-pneumatic (E/P) transducer. The complicated shear loading type (e.g., small-strain cyclic loading, sustained loading) can be achieved by the precise gear loading system. It can respond sharply to control the loading directions and speed [27].

In this study, some parts of this apparatus were improved. A pair of diaphragm pumps were used to solve the durability problem due to the long-term operation during SL test. And the heat insulator (No.② in Fig. 2) was installed below the load cell to eliminate the effect of heat transferred from the inside of the cell chamber.

3.3 Specimen Preparation

The specimen was basically cylindrical in shape (150 mm in height and 70 mm in diameter). Hostun sand sample was prepared by pluviating the sand particles through the air into a split mould,

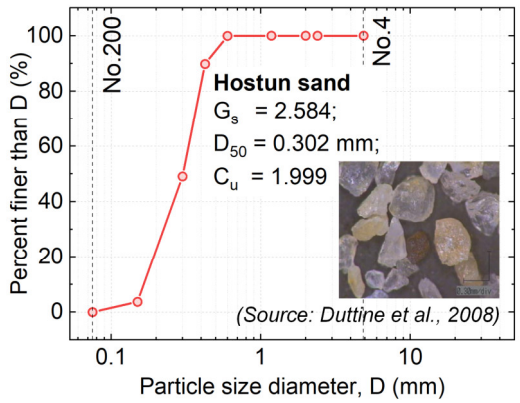

Fig. 1 Gradation curve and particle shape of Hostun sand used in present study (modified from Duttine et al. [28]

The specimen was basically cylindrical in shape (150 mm in height and 70 mm in diameter). Hostun sand sample was prepared by pluviating the sand particles through the air into a split mould, adhered which a rubber membrane to the inner surface by suction around 20 kPa. The multiple-sieving apparatus was used to achieve high uniformity. At the top cap and pedestal, a layer of silicone grease having a thickness of 50 µm is placed to reduce friction at the ends of sample [29]. After sealing the membrane with the top cap, a partial vacuuming with 20 kPa was applied to the specimen. Then, the split mould was dissembled. The specimen was left for reaching an equilibrium stage for 30 minutes (see Fig. 3). Note that the dummy load cell was installed inside the triaxial chamber to extend the length of piston. Then, the thermocouple was installed. Next, after sealing the triaxial chamber, the partial vacuuming was gradually replaced by the cell water pressure until the cell water pressure reached 20 kPa. Then, the specimen was isotropically consolidated until the confining pressure achieved 30 kPa. The next stage is drained heating stage. In this stage, the cell pressure was maintained constant at 30 kPa, while the cell water was circulated to the heater by a pair of diaphragm pumps until reaching the target temperature. After that, the waiting period was required for allowing the specimen to achieve an equilibrium. The time spent for this period was one hour (60 mins), which is verified by the developed axial strain measured during drained heating as shown in Fig. 4. Even though the cell water temperature had been kept constant at the target temperature since the first 40 minutes, the axial strain of the specimen continued to develop until reaching equilibrium.

3.4 Test Program

In this study, a comprehensive series of shear loading histories were employed to examine the elastic and creep deformation behaviours of Hostun sand. The loading type consists of two types, which can be described as follows.

Loading type a) is continuous monotonic loading (ML) at a constant strain rate. The basic strain rate is 0.075 %/min for each target temperature.

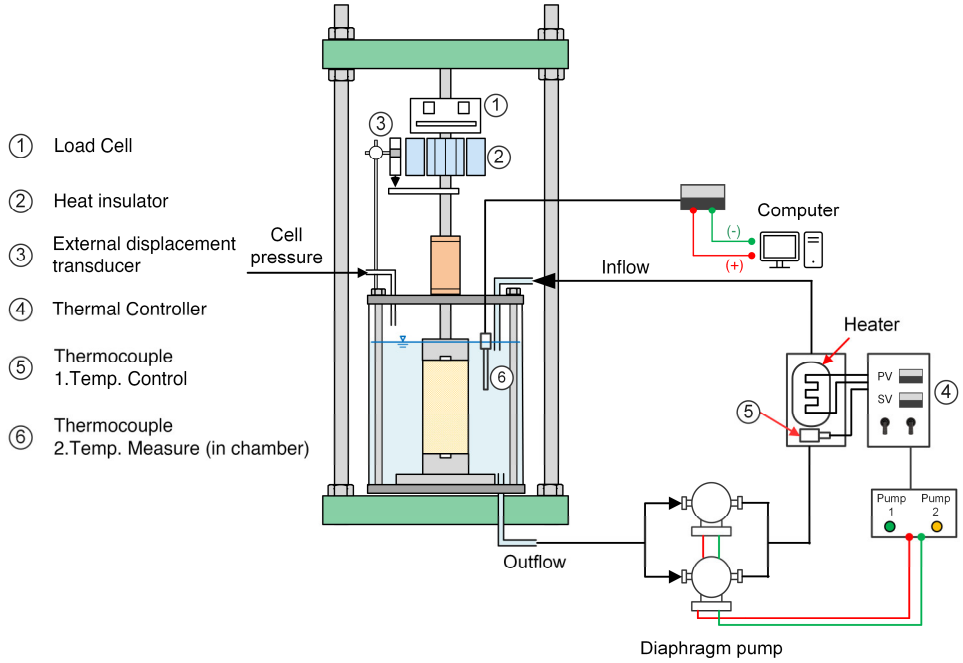

Fig. 2 Temperature-controlled triaxial compression test apparatus developed by Punya-in and Kongkitkul [20,21]

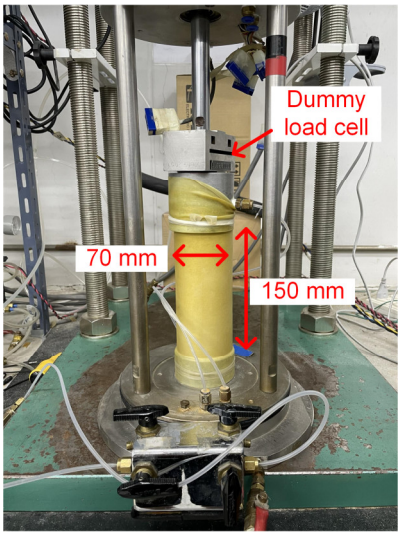

Fig. 3 Preparation of a Hostun sand sample for triaxial compression test during applying partial vacuuming of 20 kPa

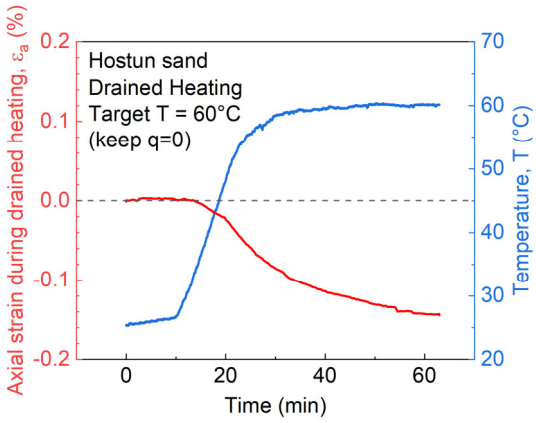

Fig. 4 Time histories of axial strain and cell water temperature during drained heating stage

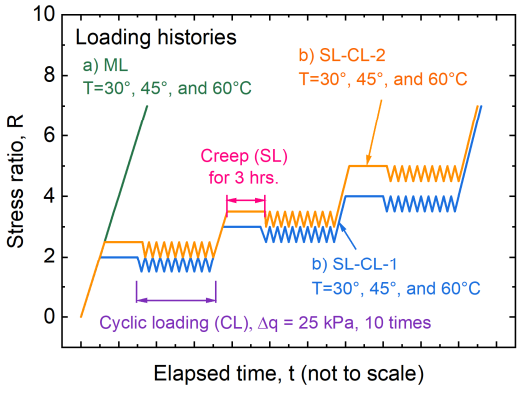

Fig. 5 Illustration of time histories of stress ratio (R) for loading types a) and b) according to the test program

Table 1 Test program and details of Hostun sand in present study

Test No.	Loading type	T (°C)	Target R	e_0 (-)	D_r (%)
1	a) ML	30	-	0.6371	86.00
2		45		0.6232	89.82
3		60		0.6503	82.37
4	b) SL-CL-1	30	2, 3, 4	0.6403	85.13
5		45		0.6395	85.35
6		60		0.6391	85.45
7	b) SL-CL-2	30	2.5, 3.5, 5	0.6426	84.49
8		45		0.6373	85.94
9		60		0.6462	83.52

Loading type b) is sustained loading and cyclic loading (SL-CL) test. It starts from ML at the basic strain rate until reaching the target stress ratio (R), which is defined as the ratio of the major to minor principal effective stresses (i.e., $R=\sigma_1'/\sigma_3'$). At the target R, SL continues for three hours to observe the creep deformation. Then, the CL with a double amplitude (Δq) of 25 kPa is applied for 10 cycles to evaluate the E_{eq}. After finishing CL, ML is restarted to the next target R value. The target R value in this loading type consists of 2.0, 2.5, 3.0, 3.5, 4.0, and 5.0. To avoid the diaphragm pump overloading, this loading type was divided into two sets using two different specimens. SL-CL tests were performed at three different R values in a single specimen as shown in Fig. 5 and listed in Table 1.

For each loading type, the cell water temperature is kept constant at either 30°C, 45°C, or 60°C throughout the shearing process. This range of temperature is consistent with the value used in the previous studies with sands by Liu et al. [13], [14], He et al. [30], and Punya-in and Kongkitkul [20,21]. Moreover, there are also limitation of the temperature-controlled triaxial testing in the present study in that: i) the cell pressure was only 30 kPa for avoiding any damage to the heater and diaphragm pumps, ii) there was no system to cool down the cell water temperature to achieve the value below the room temperature, and iii) the maximum temperature was not exceeded 60°C for avoiding any damage to the measuring devices such as pressure transducer

4. TEST RESULTS AND DISCUSSION

4.1 Influence of Temperature on Shear Strength

Figure 6 shows the relationship between stress ratio (R) and axial strain (ε_a) obtained by continuous monotonic loading (ML) (i.e., loading type a)) at constant strain rate for different temperatures. It can be readily seen that the specimens were degraded by the increasing of temperature. The shear strength of specimen can be expressed in terms of internal friction angle (ϕ), which is shown in Table 2. The ϕ values can be determined with Eq. (1) as the test sand was clean without any fines, and thus the cohesion could be assumed null. The ϕ_{peak} value is the internal friction angle at the peak state, while the ϕ_{res} value the internal friction angle at the axial strain of 14%.

$$\phi = \sin^{-1}\left(\frac{R-1}{R+1}\right) \tag{1}$$

4.2 Influence of Thermal Expansion During Drained Heating Stage

4.2.1 Determination of final void ratio after drained heating

Thermal expansion is obviously related to the change in temperature. Therefore, the thermal expansion of sand solids should partially be responsible to the temperature effects. During drained heating, the thermal expansion can occur from the solid skeleton and the air in the specimen. Due to the specimens were air-dried, the volume change could not be directly measured during drained heating. Thus, the measured axial strain was used to determine the specimen volume change. The volumetric strain ($\Delta\varepsilon_{vol}$) can be estimated from the axial strain ($\Delta\varepsilon_a$) as expressed in Eq. (2)

$$\Delta\varepsilon_{vol} \approx 3\Delta\varepsilon_a \tag{2}$$

Benjelloun et al. [31] showed that silicon dioxide (Silica, SiO_2) is the main chemical composition of Hostun sand by using the X-ray fluorescence spectrometry. Therefore, the linear thermal expansion (α) of silica sand, which is equal to $10.4\times10^{-6}/^{\circ}\mathrm{C}$, was used to calculate the volumetric thermal expansion.

During the drained heating, the volumetric thermal expansion (ΔV_s) of the sand solids can be defined as follows:

$$\Delta V_s = \beta_s (T - T_0) V_s \tag{3}$$

where β_s is the volumetric coefficient of thermal expansion of solid skeleton, V_s is the volume of the solid skeleton, T is the target temperature, and T_0 is the reference temperature, which is 30°C in this study. The β_s value can be estimated from linear thermal expansion (α) as $\beta_s \approx 3\alpha$. Thus, the β_s equal to $3.12\times10^{-5}/^{\circ}\mathrm{C}$ was used in this study. This value is nearly the same as the one reported in Liu et al. [14]. From Eqs. (2) and (3), the void ratio after drained heating can be determined by the phase calculation.

4.2.2 Internal friction angle decreased as the initial void ratio increased

As mentioned above, the thermal expansion induces the increasing of void ratio during drained heating prior to the shearing stage. From the past studies, it is known that the peak internal friction angle decreases with increasing initial void ratio (e_0) (with decreasing relative density, D_r) at the start of shearing as shown in Fig. 7. From the collected data of many studies on several sand types, a regression line of the $\phi_{peak} - D_r$ relationship can be proposed to estimate the reduction of ϕ_{peak} value by the decreasing of relative density.

Figure 8 shows the relationship between the axial strain at the equilibrium stage after drained heating and temperature. The reference temperature was equal to 30°C.

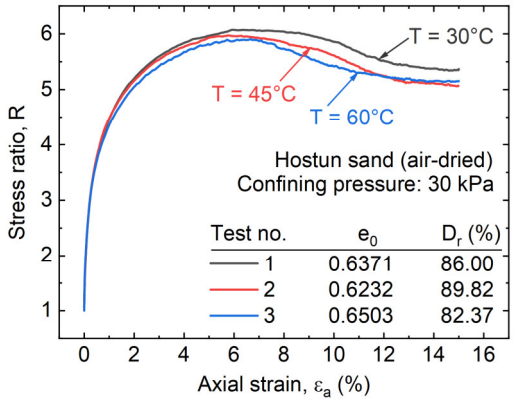

Fig. 6 $R-\varepsilon_a$ relationships by ML tests for different constant temperatures

Table 2 Internal friction angle of Hostun sand from continuous ML test with different constant temperatures

T (°C)	R_{peak}	R_{res}	ϕ_{peak} (°)	ϕ_{res} (°)
30	6.068	5.378	45.81	43.35
45	5.969	5.110	45.48	42.27
60	5.888	5.149	45.20	42.43

It can be found that the specimens were dilated by thermal expansion with a rate of -0.00656 %/°C. From this fact, the reduction of peak internal friction angle at any temperature ($\phi_{peak,T}$), can be calculated, and then the reduction of peak stress ratio (R_{peak}) can be realised.

To consider the effects of temperature increase on the reduction of strength of sand, the temperature effect (A^f) was proposed in this study, which was modified from Chantachot et al. [32,33], as expressed in Eq. (4)

$$A^f = f(T) = \frac{R_{peak} - 1}{R_{peak,0} - 1} = 1 - a\left(\frac{T - T_0}{T_0}\right)^b \quad (4)$$

where R_{peak} is the peak stress ratio at given temperature, $R_{peak,0}$ is the peak stress ratio at the reference temperature, and a and b are constant. The values of A^f obtained from i) the reduction of peak stress ratio due to the thermal expansion by the computation of changing void ratio; and ii) the peak stress ratio at given temperature by the experiment (loading type a) ML)), were plotted together against the temperature as sho[wn in Fig. 9. The thermal expansion is only a part of temperature effects. That is, the effect of temperature on the reduction of shear strength of Hostun sand cannot just simply be explained by the effect of thermal expansion. There is still a true effect of temperature existing as depicted in Fig. 9.

4.3 Stress-strain Relationship During Cyclic Loading

Figure 10 shows the relationships between stress ratio, R , and axial strain, ε_a , for loading type b) SL-CL compared with the continuous ML at temperature (T) is equal to 30°C.

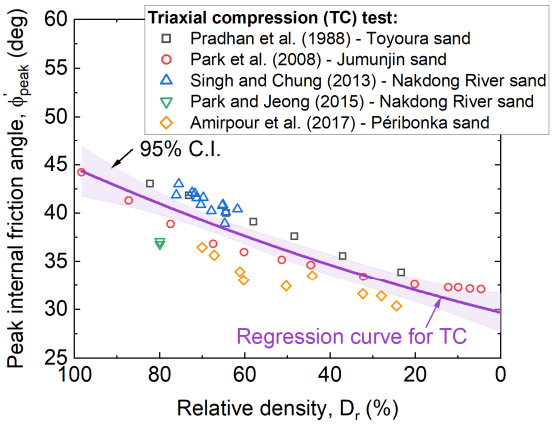

Fig. 7 Variation of peak internal friction angle with relative density of various sands collected from the literature

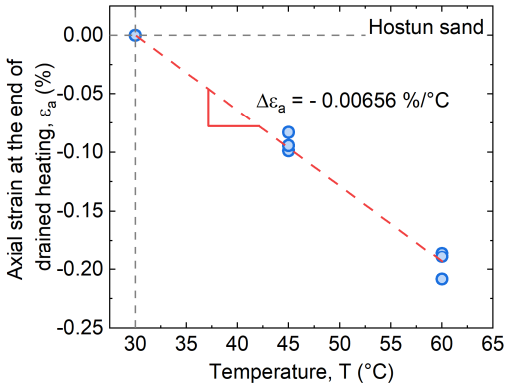

Fig. 8 Relationship between the axial strain at the end of drained heating and temperature

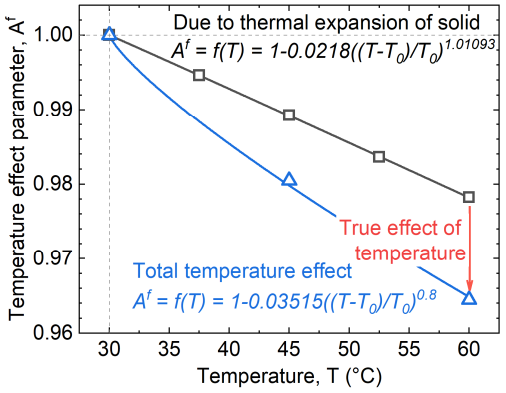

Fig. 9 Temperature effect parameter (A^f) as a function of temperature

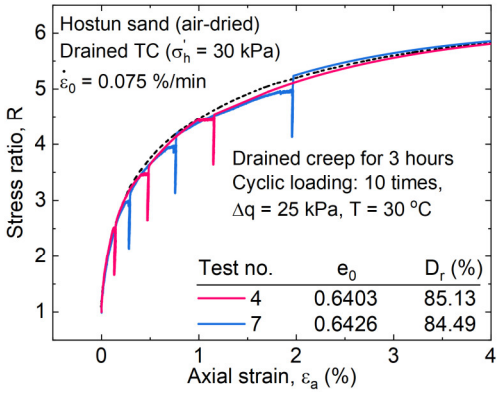

Fig. 10 $R-\varepsilon_a$ relationships with loading type b) SL-CL with $T = 30$°C

It can be found that the $R-\varepsilon_a$ relationships exhibited a high stiffness zone when the ML was restarted after completing CLs for each stress ratio. The stiffness value in this zone is very close to the elastic stiffness.

Moreover, the $R-\varepsilon_a$ relationship shows a tendency to re-join the corresponding one obtained by continuous ML tests. Therefore, it can be interpreted that the peak shear strength is maintained, or in other words, independent of loading historied applied before reaching the peak. A similar trend of behaviours can also be observed for the tests performed with the other temperatures.

4.4 Determination of Elastic Stiffness

To determine E_{eq}, the stress-strain relations during CL were re-plotted as the relationship between major principal stress (σ_1) and axial strain (ε_a). Unloading branches for the last five loops of respective CL stages were selected as shown in Fig. 11. From Fig. 11, it can be found that the unloading branch of $\sigma_1-\varepsilon_a$ relationship is quite linear, which exhibits a highly linear-elastic behaviour. The slope of this linear relation for each CL loop is the E_{eq}. The E_{eq} value is quite constant during the last five unload-reload cycles. Moreover, the R-square values obtained by linear regression were presented for respective $\sigma_1-\varepsilon_a$ relationships. This fact shows that the deformation during these unloading branches is essential elastic. The E_{eq} values from each loop were averaged for respective stress ratios, and then it was plotted in the full-log scale against the vertical stress ratio (σ_1/σ_0) for respective temperatures as shown in Fig. 12. Note that σ_0 is the reference stress equal to 100 kPa. It can be readily seen that the E_{eq} is not constant but increases with increasing stress level. This dependency of elasticity with the stress level can be expressed with Eq. (5).

$$E_{eq} = E_0\left(\sigma_1/\sigma_0\right)^m \tag{5}$$

where m is constant.

4.4.1 Comparison elastic stiffness to the previous studies

Elastic Young's modulus of standard sands at small-strain level obtained from the static method are compared together as shown in Fig. 13. Punya-in and Kongkitkul [20] investigated the elastic stiffness of a riverbed sand in Thailand by performing the temperature-controlled triaxial compression tests with varying temperatures, which are the same as the ones in this study. The increasing temperature decreases the elastic stiffness of granular materials. Hoque and Tatsuoka [16] performed TC tests on Toyoura and Hostun sands at room temperature (25°C) to evaluate the anisotropic elasticity of granular materials. The axial strain was measured by using a pair of local deformation transducers (LDTs). LDTs measure the axial deformation locally, and thus the measured value is free from bedding errors and system compliance [17]. However, due to the increasing of temperature in the chamber, it is inevitable to evaluate the axial strain by the external measurement (e.g., a linearly variable differential transformer, LVDT) for avoiding the measuring errors by the fact that the temperature alters the LDT's strain measured by the attached strain gauges. In summary, the trend of variation of E_{eq} with the stress level of Hostun sand determined in this study agrees well with the one reported in Hoque and Tatsuoka [16]. However, at the same stress level, the E_{eq} determined in this study is lower because an LVDT was used to externally measure the axial deformation, while there was no LDTs installed. Although different experimental devices were used for measuring the axial strain, the elastic properties obtained from all the collected data show that the elasticity of different granular materials is of hypo-elasticity.

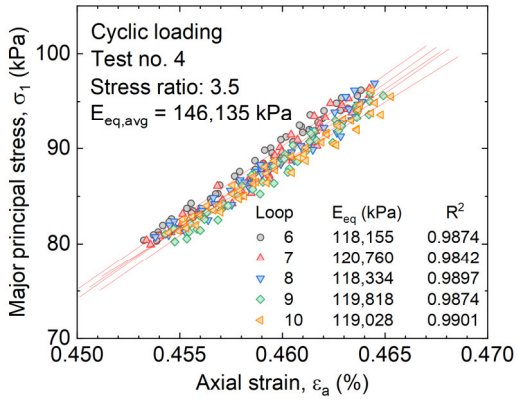

Fig. 11 $R-\varepsilon_a$ relationships during the last five unloading branches in the CL course at R = 3.5 and T = 30°C

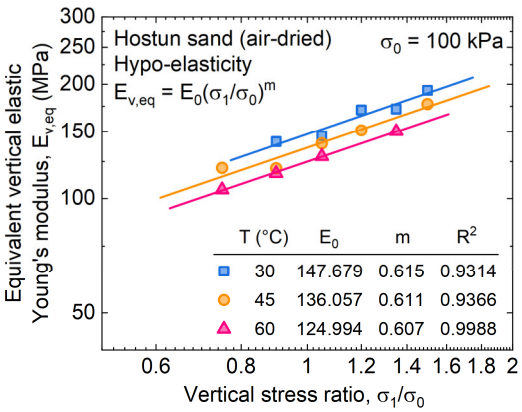

Fig. 12 Dependency of E_{eq} on the stress level and temperature with respectively fitted lines

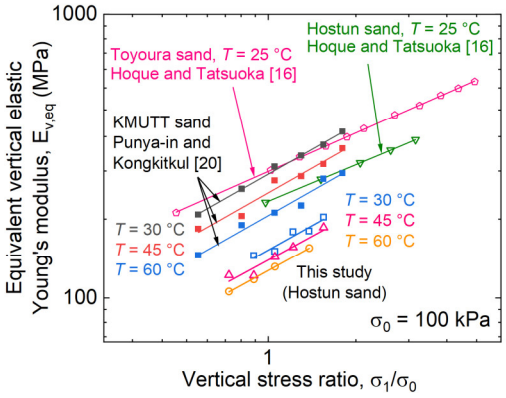

Fig. 13 Comparison of variation of E_{eq} of granular materials with the stress level and temperature

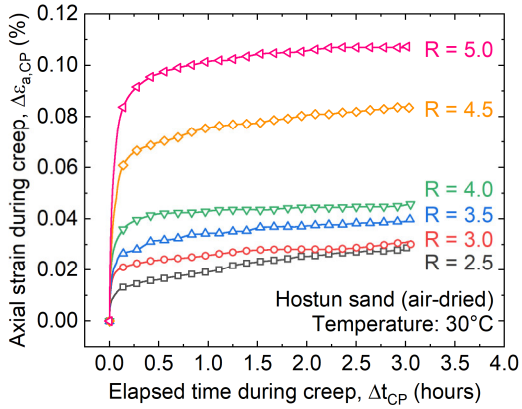

Fig. 14 Time histories of axial strain during creep by 3-hr SL at different stress ratio values with T = 30°C

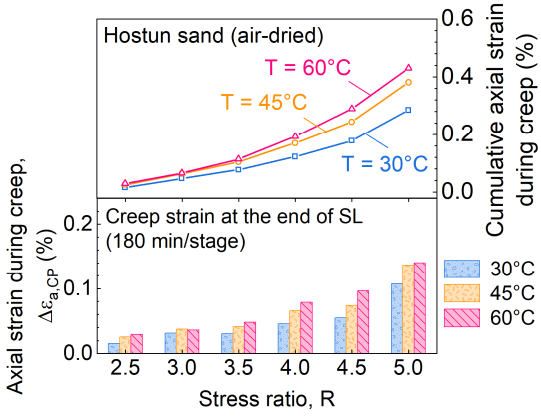

Fig. 15 Axial strain at the end of 3-hr creep and its cumulative for respective stress ratio values and different target temperatures

4.5 Creep Deformation with Temperature Changes

Figure 14 shows the time histories of axial strain during creep for 3 hours at different stress ratio values for the temperature of 30°C. It can be obviously seen that the creep strain increases with increasing stress level. Moreover, Fig. 15 presents the axial strain at the end of SL (3 hours) for different stress ratio values and different temperatures together with its cumulative. It can be found that not only the stress level but also the temperature affects an increase in the creep strain. However, the influence of stress level is much more than that of temperature.

5. CONCLUSIONS

The following conclusions can be derived from the results of temperature-controlled triaxial compression tests on Hostun sand performed in this study.

1. The peak internal friction angle decreases with increasing temperature.
2. Thermal expansion induces the dilation of sand solids when drained heating, which results in an increase in the initial void ratio before shearing and thus a reduction of the shear strength. However, its influence is only a part of temperature effects on the reduction of shear strength.
3. Elastic stiffness of Hostun sand clearly increases with increasing stress level, which is of hypo-elastic. Moreover, at the same stress level, the elastic stiffness decreases with increasing temperature.
4. Creep strain increases with increasing stress level and temperature. However, the influence of stress level on the creep strain development seems to be more dominant than that of temperature.

6. ACKNOWLEDGMENTS

The authors are grateful to King Mongkut's University of Technology Thonburi (KMUTT) for the financial support granted to this research via The Petchra Pra Jom Klao PhD scholarship under contract Grant No. 7/2563. The authors would like to extend the appreciation to the Prof. Fumio Tatsuoka and Prof. Yoshiaki Kikuchi, Tokyo University of Science (TUS), Japan and Prof. Reiko Kuwano, Institute of Industrial Science (IIS), University of Tokyo, Japan for supporting the Hostun sand and other granular materials.

7. REFERENCES

[1] Brandl H., Energy foundations and other thermo-active ground structures. Geotechnique, Vol.56, No. 2, 2006, pp. 81-122.

[2] Knellwolf C., Peron H., and Laloui L., Geotechnical Analysis of Heat Exchanger Piles, Journal of Geotechnical and Geoenvironmental Engineering, Vol.137, No.10, 2011, pp. 890-902.

[3] Olgun C. G., Ozudogru T. Y., and Arson C. F., Thermo-mechanical radial expansion of heat exchanger piles and possible effects on contact pressures at pile-soil interface, Geotechnique Letters, Vol.4, 2014, pp. 170-178.

[4] Moradshahi A., Faizal M., Bouazza A., and McCartney J. S., Effect of nearby piles and soil properties on thermal behaviour of a field-scale energy pile, Canadian Geotechnical Journal, Vol.58, No.9, 2021, pp. 1351-1364.

[5] Zymnis D. M. and Whittle A. J., Geotechnical considerations in the design of borehole heat exchangers, Canadian Geotechnical Journal, Vol.58, No.9, 2021, pp. 1247-1262.

[6] Stewart, M. A., Coccia C. J., and McCartney J. S. Issues in the implementation of sustainable heat exchange technologies in reinforced, unsaturated soil structures, in Geo-Congress 2014: Geo-characterization and Modeling for Sustainability, 2014, pp. 4066-4075.

[7] Gens A., Sanchez M., Guimaraes L. D., Alonso E. E., Lloret A., Olivella S., Villar M. V., and Huertas F., A full-scale in situ heating test for high-level nuclear waste disposal: observations, analysis and interpretation, Geotechnique, Vol.59, No.4, 2009, pp. 377-399.

[8] De Bruyn D. and Thimus J.-F., The influence of temperature on mechanical characteristics of Boom clay: the results of an initial laboratory programme, Engineering Geology, Vol.41, No.1, 1996, pp. 117-126.

[9] Cekerevac C. and Laloui L., Experimental study of thermal effects on the mechanical behaviour of a clay, International Journal for Numerical and Analytical Methods in Geomechanics, Vol.28, No.3, 2004, pp. 209-228.

[10] Abuel-Naga H., Bergado D., Ramana G., Grino L., Rujivipat P., and Thet Y., Experimental evaluation of engineering behavior of soft Bangkok clay under elevated temperature, Journal of geotechnical and geoenvironmental engineering, Vol.132, No.7, 2006, pp. 902-910.

[11] Tsutsumi A. and Tanaka H., Combined effects of strain rate and temperature on consolidation behavior of clayey soils, Soils and Foundations, Vol.52 No.2, 2012, pp. 207-215.

[12] Graham J., Alfaro M., and Ferris G., Compression and strength of dense sand at high pressures and elevated temperatures, Canadian Geotechnical Journal, Vol.41, No.6, 2004, pp. 1206-1212.

[13] Liu H., Liu H., Xiao Y., and McCartney J. S., Effects of temperature on the shear strength of saturated sand, Soils and Foundations, 2018, Vol.58, No.6, 2018, pp. 1326-1338.

[14] Liu H., Liu H., Xiao Y., and McCartney J. S., Influence of Temperature on the Volume Change Behavior of Saturated Sand, Geotechnical Testing Journal, 2018. Vol.41, No.4, 2018, pp. 747-758.

[15] Tatsuoka F., Inelastic deformation characteristics of geomaterial, in Soil stress-strain behavior: measurement, modeling and analysis, Springer, Dordrecht, 2007, pp. 1-108.

[16] Hoque E. and Tatsuoka F., Anisotropy in Elastic Deformation of Granular Materials, Soils and Foundations, Vol.38, No.1, 1998, pp. 163-179.

[17] Kohata Y., Tatsuoka F., Wang L., Jiang G., Hoque E., and Kodaka T., Modelling the non-linear deformation properties of stiff geomaterials, Geotechnique, Vol.47, No.3, 1997, pp. 563-580.

[18] Duttine A., Di Benedetto H., Pham Van Bang D., and Ezaoui A., Anisotropic Small Strain Elastic Properties of Sands and Mixture of Sand-clay Measured by Dynamic and Static Methods, Soils and Foundations, Vol.47, No.3, 2007, pp. 457-472.

[19] Mitchell J. K., Temperature effects on the engineering properties and behavior of soils, Highway Research Board Special Report, Vol.103, 1969, pp. 9-28.

[20] Punya-in Y. and Kongkitkul W., Effects of temperature on the stress-strain-time behavior of sand under shear, Journal of Testing and Evaluation, Vol.51, No.2, 2022, pp. 1-21.

[21] Punya-in Y. and Kongkitkul W., Effects of Temperature on Equivalent Elastic and Creep Deformation Behaviors of a Dried Sand, International Journal of GEOMATE, Vol.22, Issue 90, 2022, pp. 1-9.

[22] Murayama S., Effect of temperature on elasticity of clays, in Effects of Temperature and Heat on Engineering Properties of Soils, Spacial Report 103, Highway research board, Issue.103, 1969, pp. 194-203.

[23] Enomoto T., Kawabe S., Tatsuoka F., Di Benedetto H., Hayashi T., and Duttine A., Effects of particle characteristics on the viscous properties of granular materials in shear, Soils and Foundations, Vol.49, No.1, 2009, pp. 25-49.

[24] Tatsuoka F., Di Benedetto H., Enomoto T., Kawabe S., and Kongkitkul W., Various viscosity types of geomaterials in shear and their mathematical expression, Soils and

Foundations, Vol.48, No.1, 2008, pp. 41-60.
[25] Kaddouri Z., Cuisinier O., and Masrouri F., Influence of effective stress and temperature on the creep behavior of a saturated compacted clayey soil, Geomechanics for Energy and the Environment, Vol.17, 2019, pp. 106-114.
[26] Japanese Standards Association, Test method for minimum and maximum densities of sands (JIS A 1224: 2009). Japanese Industrial Standards, Tokyo, Japan, 2009. (in Japanese)
[27] Santucci de Magistris F., Koseki J., Amaya M., Hamaya S., Sato T., and Tatsuoka F., A triaxial testing system to evaluate stress-strain behavior of soils for wide range of strain and strain rate, Geotechnical Testing Journal, Vol.22, No.1, 1999, pp. 44-60.
[28] Duttine A., Tatsuoka F., Kongkitkul W., and Hirakawa D., Viscous behaviour of unbound granular materials in direct shear, Soils and Foundations, Vol.48, No.3, 2008, pp. 297-318.
[29] Tatsuoka F. and Haibara O., Shear resistance between sand and smooth or lubricated surfaces, Soils and Foundations, Vol.25, No.1, 1985, pp. 89-98.
[30] He S. H., Shan H. F., Xia T. D., Liu Z. J., Ding Z., and Xia F., The effect of temperature on the drained shear behavior of calcareous sand, Acta Geotechnica, Vol.16, No.2, 2021, pp. 613-633.
[31] Benjelloun M., Bouferra R., Ibouh H., Jamin F., Benessalah I., and Arab A., Mechanical Behavior of Sand Mixed with Rubber Aggregates, Applied Sciences, Vol.11, No.23, 2021, pp. 1-19.
[32] Chantachot, T., Kongkitkul W., and Tatsuoka F., Effects of temperature rise on load-strain-time behaviour of geogrids and simulations. Geosynthetics International, Vol.25, No.3, 2018, pp. 287-303.
[33] Chantachot T., Kongkitkul W., and Tatsuoka F., Effects of Temperature on Elastic Stiffness of a HDPE Geogrid and Its Model Simulation, International Journal of GEOMATE, Vol. 12, Issue 32, 2016, pp. 94-100